Mercury sources, distribution, and bioavailability in the North Pacific Ocean: Insights from data and models

Elsie M. Sunderland,[1] David P. Krabbenhoft,[2] John W. Moreau,[3] Sarah A. Strode,[4] and William M. Landing[5]

Received 14 November 2008; revised 26 January 2009; accepted 2 February 2009; published 1 May 2009.

[1] Fish harvested from the Pacific Ocean are a major contributor to human methylmercury (MeHg) exposure. Limited oceanic mercury (Hg) data, particularly MeHg, has confounded our understanding of linkages between sources, methylation sites, and concentrations in marine food webs. Here we present methylated (MeHg and dimethylmercury (Me_2Hg)) and total Hg concentrations from 16 hydrographic stations in the eastern North Pacific Ocean. We use these data in combination with information from previous cruises and coupled atmospheric-oceanic modeling results to better understand controls on Hg concentrations, distribution, and bioavailability. Total Hg concentrations (average 1.14 ± 0.38 pM) are elevated relative to previous cruises. Modeling results agree with observed increases and suggest that at present atmospheric Hg deposition rates, basin-wide Hg concentrations will double relative to circa 1995 by 2050. Methylated Hg accounts for up to 29% of the total Hg in subsurface waters (average 260 ± 114 fM). We observed lower ambient methylated Hg concentrations in the euphotic zone and older, deeper water masses, which likely result from decay of MeHg and Me_2Hg when net production is not occurring. We found a significant, positive linear relationship between methylated Hg concentrations and rates of organic carbon remineralization ($r^2 = 0.66$, $p < 0.001$). These results provide evidence for the importance of particulate organic carbon (POC) transport and remineralization on the production and distribution of methylated Hg species in marine waters. Specifically, settling POC provides a source of inorganic Hg(II) to microbially active subsurface waters and can also provide a substrate for microbial activity facilitating water column methylation.

Citation: Sunderland, E. M., D. P. Krabbenhoft, J. W. Moreau, S. A. Strode, and W. M. Landing (2009), Mercury sources, distribution, and bioavailability in the North Pacific Ocean: Insights from data and models, *Global Biogeochem. Cycles*, *23*, GB2010, doi:10.1029/2008GB003425.

1. Introduction

[2] Consuming fish elevated in methylmercury (MeHg) causes adverse human health effects ranging from neurodevelopmental deficits in children to increased risk of myocardial infarction in adults [*Mergler et al.*, 2007; *NRC*, 2000]. Globally, most fish and shellfish for human consumption are harvested from marine and estuarine systems (Yearbook summary tables: Capture, aquaculture and commodity fishery statistics, in FAO Yearbook of Fisheries Statistics, FAO, U. N., Rome, 2007, available at http://www.fao.org/fishery/statistics/programme/3,1,3). The Pacific Ocean supplies more than 60% of the global tuna harvest, which accounts for approximately 40% of U.S. population-wide Hg intake [*Sunderland*, 2007]. Despite the importance of marine systems for human exposure, previous studies of oceanic Hg distribution and bioavailability are extremely limited. Here we present the first methylated Hg (MeHg and dimethylmercury (Me_2Hg)) concentration data for the North Pacific Ocean measured using clean sampling and analytical techniques [*Gill and Fitzgerald*, 1987]. Methylmercury is the only species that bioaccumulates in aquatic food webs and is also the major product of Me_2Hg decomposition in marine systems [*Wiener et al.*, 2003; *Whalin et al.*, 2007]. Here we examine controls on oceanic Hg distribution and speciation using new chemical and physical oceanographic data combined with measurements from previous cruises and coupled atmospheric-oceanic Hg cycling models.

[3] Physical, chemical and biological properties of oceans all play a role in determining the relative abundance of the four main Hg species in seawater: divalent inorganic mercury (Hg(II)), elemental mercury (Hg(0)), Me_2Hg, and MeHg [*Mason and Fitzgerald*, 1993]. Speciated Hg data are critical

[1]School of Engineering and Applied Sciences, Harvard University, Cambridge, Massachusetts, USA.
[2]U.S. Geological Survey, Middleton, Wisconsin, USA.
[3]School of Earth Sciences, University of Melbourne, Melbourne, Australia.
[4]Department of Atmospheric Sciences, University of Washington, Seattle, Washington, USA.
[5]Department of Oceanography, Florida State University, Tallahassee, Florida, USA.

0886-6236/09/2008GB003425$12.00

for understanding the fate of atmospherically deposited anthropogenic Hg and resulting impacts on biological exposure levels. For example, *Mason and Fitzgerald* [1991] first hypothesized that the amount of bioavailable Hg in the ocean reflects the balance between reduction and methylation of Hg(II).

[4] Anticipating how MeHg levels in pelagic marine fish will change over time requires an understanding of the primary MeHg sources for marine food webs (e.g., atmospheric deposition, advection and diffusion from deep ocean sediments, and/or ocean margins). For example, preliminary modeling suggests water column methylation processes will result in more rapid changes in biologically available Hg than deep ocean sediment sources [*Kraepiel et al.*, 2003; *Mason and Gill*, 2005]. Previous research shows that MeHg production in freshwater and estuarine water and sediments mainly occurs through biologically mediated conversion of Hg(II) under geochemically favorable conditions (e.g., low oxygen, labile carbon) by anaerobic bacteria such as some sulfate and iron reducers [*Benoit et al.*, 2003; *Eckley and Hintelmann*, 2006; *Hammerschmidt and Fitzgerald*, 2004; *Kerin et al.*, 2006; *Sunderland et al.*, 2004; 2006]. Several studies have postulated that MeHg produced in ocean margin sediments and bioadvected (with plankton and fish) and/or horizontally transported along isopycnal surfaces to open ocean regions is the primary Hg source for predatory marine fish [*Hammerschmidt and Fitzgerald*, 2006a; 2006b]. However, recent data showing active Hg methylation in the marine water column [*Ekstrom et al.*, 2006; *Kirk et al.*, 2008; *Monperrus et al.*, 2007a; 2007b; *St. Louis et al.*, 2007] suggest that MeHg entry into marine food webs may not depend on a link to sediment MeHg and/or benthic food chains as previously hypothesized [*Kraepiel et al.*, 2003]. Here we examine evidence for in situ water column Hg methylation in the North Pacific by investigating relationships between observed methylated Hg distributions and ancillary hydrographic and nutrient data.

[5] Atmospheric deposition is widely recognized as the dominant Hg source to open ocean regions [*Mason and Sheu*, 2002]. Concentrations in the shallow (50–150 m) surface mixed layer rapidly reach steady state with atmospheric Hg inputs but intermediate and deep ocean waters respond on timescales ranging from decades to centuries [*Strode et al.*, 2007; *Sunderland and Mason*, 2007]. Over the past 2 decades anthropogenic Hg emissions have declined in North America and Europe but increased substantially (~2×) in East Asia and India [*Pacyna et al.*, 2006]. Despite these emissions increases, after examining data from several sampling campaigns, *Laurier et al.* [2004] found that Hg concentrations in the North Pacific Ocean did not change substantially between 1980 and 2002. Here we revisit this hypothesis by comparing more recent (2006) measurements to all previous cruise data from the eastern North Pacific Ocean.

[6] The objectives of this study are to better understand biogeochemical controls on methylated Hg production and distribution in open ocean environments and to investigate temporal trends in total Hg concentrations the North Pacific Ocean. To do this, we examine relationships between methylated Hg data, nutrients (and other indicators of biological productivity), and several proxies for organic carbon remineralization and heterotrophic activity in the water column. To assess temporal trends in North Pacific Hg concentrations, we quantify sources and rates of atmospheric Hg deposition using tagged tracer results from a global-scale model (GEOS-Chem) [*Strode et al.*, 2008]. We also use modeled Hg concentration changes in intermediate ocean waters using a multicompartment global ocean box model [*Sunderland and Mason*, 2007]. We compare modeling results to measured Hg levels in surface and intermediate waters from this study and previous cruises to gain insight into past and future Hg concentration trends.

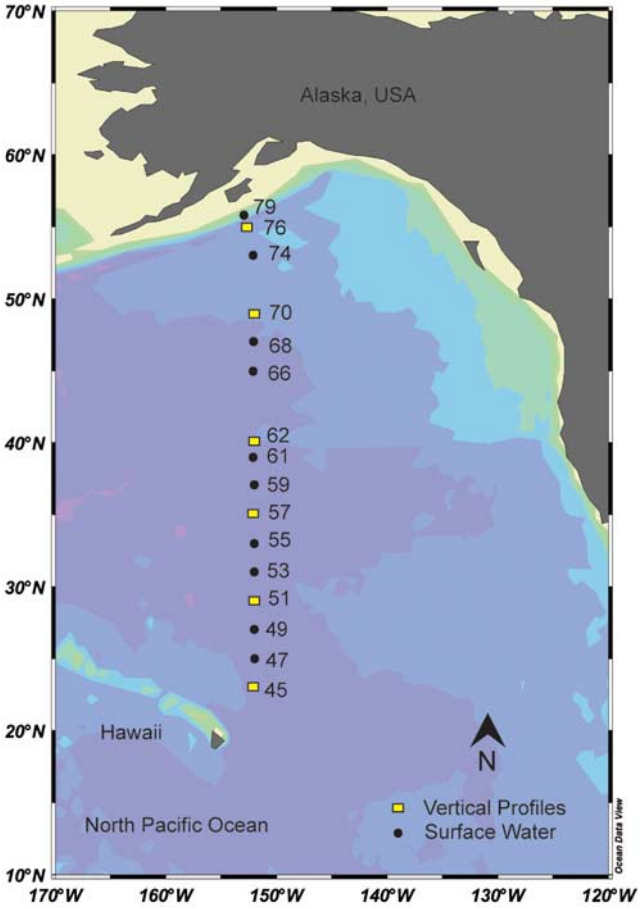

Figure 1. Locations of hydrographic stations sampled for mercury along the CLIVAR P16N Leg-2 cruise track from Honolulu, Hawaii, and Kodiak, Alaska, United States, from 10–30 March 2006 (Chief Scientist: Richard A. Feely).

2. Methods

2.1. Sampling

[7] Samples were collected during the second half of a hydrographic survey of the eastern North Pacific Ocean (P16N Leg-2) from 10–30 March 2006 on the vessel *R/V Thomas G. Thompson*. The cruise nominally followed a 152°W transect between Honolulu, Hawaii, and Kodiak, Alaska, United States (Figure 1). The P16N Leg 2 cruise is part of a decadal series of repeat hydrography sections jointly funded by the NOAA Office of Global Programs

(now the Climate Program Office) and the National Science Foundation Division of Ocean Sciences as part of the Climate Variability and Predictability Study (CLIVAR) CO_2 Repeat Hydrography Program. A total of 41 stations were occupied and samples for Hg analysis were collected at 16 stations (Figure 1). Vertical profiles to a depth of 1000 m were obtained at six stations and surface samples ($\sim$20 m depth) were collected at ten stations (Figure 1). A specially designed apparatus consisting of 12–12 L Teflon-lined Go-Flo bottles mounted on a powder-coated rosette frame was used to collect all samples [*Measures et al.*, 2008]. All Go-Flo bottles were cleaned prior to sample collection by repeated flushing with seawater. Samples for Hg analysis were decanted from the Go-Flo bottles into acid-washed Teflon bottles under clean laboratory conditions, acidified using dilute OmniTrace ultrapure HCl within 60 min of collection, and stored for laboratory analysis on shore. A side-by-side comparison of all sampling methods, procedures and instruments used on the P16N cruise and those employed in previous studies of the North Pacific was performed in the Atlantic Ocean in 2008. This comparison resulted in no significant differences in measured Hg concentrations (R. Mason, personal communications, 2008).

2.2. Ancillary Hydrographic Data Collection

[8] Basic hydrographic measurements at all stations included salinity, dissolved oxygen and nutrients. For each of the 41 stations occupied, thirty-six 12L Niskin-type bottles were used to collect samples from throughout the water column. Each Niskin was subsampled on deck for a variety of analyses. Nutrient samples were collected from the Niskin bottles in acid washed 25-mL linear polyethylene bottles after three complete seawater rinses and analyzed within 1 h of sample collection. Measurements were made in a temperature-controlled laboratory (20 ± 2°C). Concentrations of nitrite (NO_2^-), nitrate (NO_3^-), phosphate (PO_4^{3-}) and silicic acid (H_4SiO_4) were determined using an Alpkem Flow Solution Auto-Analyzer aboard the ship. Further details of carbon data collection and analysis [*Sabine et al.*, 2008] and methods used to collect and analyze ancillary hydrographic data are reported elsewhere [*Feely et al.*, 2006].

2.3. Total Hg Analysis

[9] All Hg and MeHg analyses were performed at the USGS Mercury Research Laboratory in Middleton, Wisconsin (http://wi.water.usgs.gov/mercury-lab/). Total Hg analysis followed U.S. EPA Method 1631. Aqueous samples were pretreated by the addition of 1–2 percent (v/v) 0.2 N Bromine monochloride (BrCl) to solubilize and oxidize all forms of Hg to reactive mercuric ion (Hg^{2+}). Samples were placed in an oven at 50°C for a minimum of 12 h to accelerate the oxidation reaction. Oxidation was considered complete when excess BrCl was present, detectable by a faint yellow color. Immediately prior to analysis, a small amount of hydroxylamine hydrochloride (NH_2OH–HCl) was added to each sample until the residual color from added BrCl disappeared. Approximately 10 min after BrCl reduction, 0.5 ml of stannous chloride ($SnCl_2$) was added to the sample within the bubbling flask to reduce the Hg^{2+} to Hg(0). The Hg(0) was purged from samples with Hg-free N_2 gas and concentrated onto a gold-coated, glass bead trap. Finally, gold traps were heated and the Hg(0) thermally desorbed into an Argon gas stream and quantified by cold vapor atomic fluorescence spectroscopy (CVAFS). The daily detection limit (DDL) for these specific analytical runs during total Hg analysis was 0.06 pM and the precision, measured as the relative percent difference (RPD) between analytical duplicates, averaged 10% (n = 11 pairs).

2.4. Methylmercury Analysis

[10] Previous studies have shown that Me_2Hg is unstable and will rapidly decompose into MeHg in acidified samples. For example, *Mason and Sullivan* [1999] estimated a degradation rate of $0.2 - 2.0 \times 10^{-5}$ s^{-1} in the presence of light. Since Me_2Hg concentrations were not analyzed on board the cruise, all ''methylated Hg'' measurements reported here refer to the combined concentrations of Me_2Hg and MeHg.

[11] Methylmercury analyses were performed following standard distillation and ethylation procedures described in detail elsewhere [*De Wild et al.*, 2002; *Horvat et al.*, 1993]. In addition, we added precise quantities of MeHg isotope ($Me^{199}Hg$) to all samples to assess recoveries on an individual basis. Briefly, this method calls for isolation of all ambient MeHg and amended $Me^{199}Hg$ from the sample matrix by atmospheric pressure water vapor distillation. The MeHg in the distillates was derivatized using sodium tetraethylborate and preconcentrated onto Carbo traps. Detection and quantification was achieved after thermodesorption, isothermic GC separation, and detection by ICP/MS [*Hintelmann and Evans*, 1997]. Approximately 30 min before the distillation, 30 picograms of $Me^{199}Hg$ were added to each sample to serve as a sample-specific internal standard. Because detection was performed using an ICP/MS, the $Me^{199}Hg$ was quantified independently from the ambient MeHg. Following $Me^{199}Hg$ analysis, all other Hg isotope masses were corrected on the basis of the internal standard recovery ratio. Across all samples, recoveries averaged 101 ± 5%. Individually applied recoveries help to correct for variability commonly observed for spike addition checks on performance, random errors associated with derivatization, and detection steps, as well as drifts in instrument response. The daily detection limit using the combined method with isotope dilution was 0.05 pM. Precision, measured as the relative percent difference (RPD) between analytical duplicates, averaged 20% (n = 11 pairs).

2.5. Organic Carbon Remineralization Rates and Associated Data

[12] Several previous studies have proposed relationships among Hg methylation, biological productivity, and organic matter settling and decomposition in open ocean environments [*Mason et al.*, 1998; *Mason and Fitzgerald*, 1993; *Monperrus et al.*, 2007a]. We used cruise data collected here to calculate several proxy indicators of water column productivity and organic carbon decomposition. These include remineralized carbon concentrations (C_{rm}, μmol kg^{-1}), apparent oxygen utilization (AOU, μmol kg^{-1}), and the organic carbon remineralization rate ($OCRR$, μmol kg^{-1} a^{-1}).

[13] Biogeochemical utilization of oxygen, carbon and nutrients during organic carbon decomposition in marine

Table 1. Linear Relationships Between Measured Total Carbon and Nitrate, Phosphate, and Silicate Concentrations[a]

TC Predictor	Slope (±1 stdev)	Intercept (±1 stdev)	Correlation Coefficient (r^2)	Significance
Nitrate	7.9 ± 0.60	1997 ± 21	0.96	$p < 0.001$
Phosphate	120 ± 8.8	1991 ± 21	0.96	$p < 0.001$
Silicate	2.5 ± 0.18	2067 ± 16	0.96	$p < 0.001$

[a]All units for carbon and nutrients are μmol kg^{-1}. TC, total carbon.

waters are well characterized by a series of coefficients better known as Redfield ratios [*Anderson and Sarmiento*, 1994; *Redfield et al.*, 1963; *Takahashi et al.*, 1985]. Some phytoplankton, such as diatoms, also require silica, which can provide a substrate for downward flux of organic matter, enhancing remineralization [*Feely et al.*, 2004]. Changes in total carbon with depth mainly reflected the addition of remineralized carbon through particulate organic carbon (POC) decomposition [*Lee*, 2001; *Millero*, 2006]. Similarly, total carbon concentrations measured on the P16N cruise are linearly related to nitrate, phosphate and silicate concentrations, reflecting the relatively constant ratios of these nutrients released to the water column during POC remineralization (Table 1). We derived four estimates of total carbon in intermediate waters sampled on the P16N cruise using directly measured total carbon concentrations and linear relationships with nutrients shown in Table 1.

[14] Total carbon includes both inorganic ($[CO_2]$ + $[HCO_3^-]$ + $[CO_3^{2-}]$) and dissolved organic carbon (DOC) [*Millero*, 2006]. The DOC fraction makes up less than 2% of the total carbon in the eastern North Pacific (range 35–38 μmol kg^{-1} across all stations) and therefore does not substantially affect vertical distributions. We estimated C_{rm} by subtracting average inorganic carbon concentrations in surface waters (approximately 2050 μmol kg^{-1}, corrected for salinity) from total carbon concentrations measured in intermediate waters [*Feely et al.*, 2004; *Millero*, 2006]. Although the majority of C_{rm} is from POC decomposition, on average calcium carbonate ($CaCO_3$) dissolution accounts for 6% of the remineralized carbon in Pacific Ocean waters and this fraction varies with depth [*Feely et al.*, 2004].

[15] Because of the potentially confounding effects of inorganic carbon dissolution and water mass circulation on C_{rm}, we used *AOU* and *OCRR* as additional indicators of organic carbon decomposition and associated heterotrophic activity. The *AOU* is the difference between solubility of oxygen at a given temperature and salinity and measured water column concentrations, reflecting biological demand for oxygen during decomposition of organic matter [*Weiss*, 1970]. We derived *AOU* using measured oxygen concentrations and solubility equations and constants from *Garcia and Gordon* [1992]. Water mass circulation means that *AOU* does not necessarily reflect in situ organic carbon remineralization rates [*Najjar et al.*, 2007]. Therefore, we calculated *OCRR* using the model by *Feely et al.* [2004]:

$$OCRR = \Delta C_{org}/AGE = R_{C:O}{}^{*}AOU/AGE \quad (1)$$

where ΔC_{org} is the change in organic carbon related to *AOU* by the product of the biogeochemical utilization of oxygen during organic carbon decomposition (e.g., the C:O Redfield ratio for the Pacific, $R_{C:O} = 0.688$) [*Anderson and Sarmiento*, 1994]. We calculated organic carbon concentrations (ΔC_{org}) by the difference between measured total carbon concentrations in surface and intermediate waters, and by subtracting the amount of remineralized inorganic carbon from $CaCO_3$ dissolution. We estimated the amount of dissolved $CaCO_3$ in each sample using the relationship between the ratios of C_{org}:C_{inorg} ($CaCO_3$) dissolution and depth for the North Pacific reported by *Feely et al.* [2004]. We calculated the "apparent age" (*AGE*, years) of intermediate waters using the pCFC-12 values measured on the P16N cruise. Apparent ages reflect the average age of the water mass through both mixing with older waters and the time since the water mass outcropped at the surface [*Doney and Bullister*, 1992; *Wisegarver and Gammon*, 1988]. The known solubility of CFC-12 at a given temperature and salinity can be used to relate measured concentrations in seawater to an equivalent concentration in air, which corresponds to a specific time period [*Watanabe et al.*, 2003; *Wisegarver and Gammon*, 1988]. We used the salinity and temperature specific solubility tables for CFC-12 from *Warner and Weiss* [1985] and the atmospheric time history of CFC concentrations from *Watanabe et al.* [2003] to estimate the *AGE* of intermediate water masses sampled in this study.

[16] Rates of organic carbon remineralization (*OCRR*) calculated here fall within ranges produced by *Feely et al.* [2004]. We found average *OCRR*s of 5.28 ± 1.31 and 3.79 ± 1.70 μmol kg^{-1} a^{-1} in the Pacific Subarctic Water mass and North Pacific Central/Intermediate Waters, respectively, compared to 0.01–6.4 μmol kg^{-1} a^{-1} in the Pacific Subarctic Upper Water and 0.04–4.0 μmol kg^{-1} a^{-1} in the North Pacific Central Water from *Feely et al.* [2004].

2.6. Atmospheric/Oceanic Modeling

[17] Atmospheric Hg deposition and source attribution information reported here are from simulations performed using the GEOS-Chem global tropospheric chemistry transport model version 7.04 (http://www-as.harvard.edu/chemistry/trop/geos/), adapted for Hg by *Selin et al.* [2007]. Source attribution results are based on tracer simulations for Hg(0), Hg(II) and particulate mercury (Hg(P)) described in *Strode et al.* [2008]. For these simulations, the model has a horizontal resolution of 2° latitude by 2.5° longitude, 30 vertical layers, and uses assimilated meteorology from the NASA Global Modeling and Assimilation Office (GMAO). The atmospheric model is fully coupled with a slab model of the ocean surface mixed layer [*Strode et al.*, 2007]. Simulations are based on contemporary global anthropogenic Hg emissions estimates [*Pacyna et al.*, 2006; *Wilson et al.*, 2006], biomass burning, natural emissions, and reemissions from land and the ocean. Additional details of the atmospheric model formulation and parameterization can be found in *Selin et al.* [2008] and *Strode et al.* [2008].

[18] We modeled the trajectory of Hg concentrations in North Pacific intermediate waters over several decades using the multicompartment global ocean box model developed by *Sunderland and Mason* [2007] and contemporary atmospheric deposition from the GEOS-Chem model. The ocean model is based on the simplified physical framework for transport and

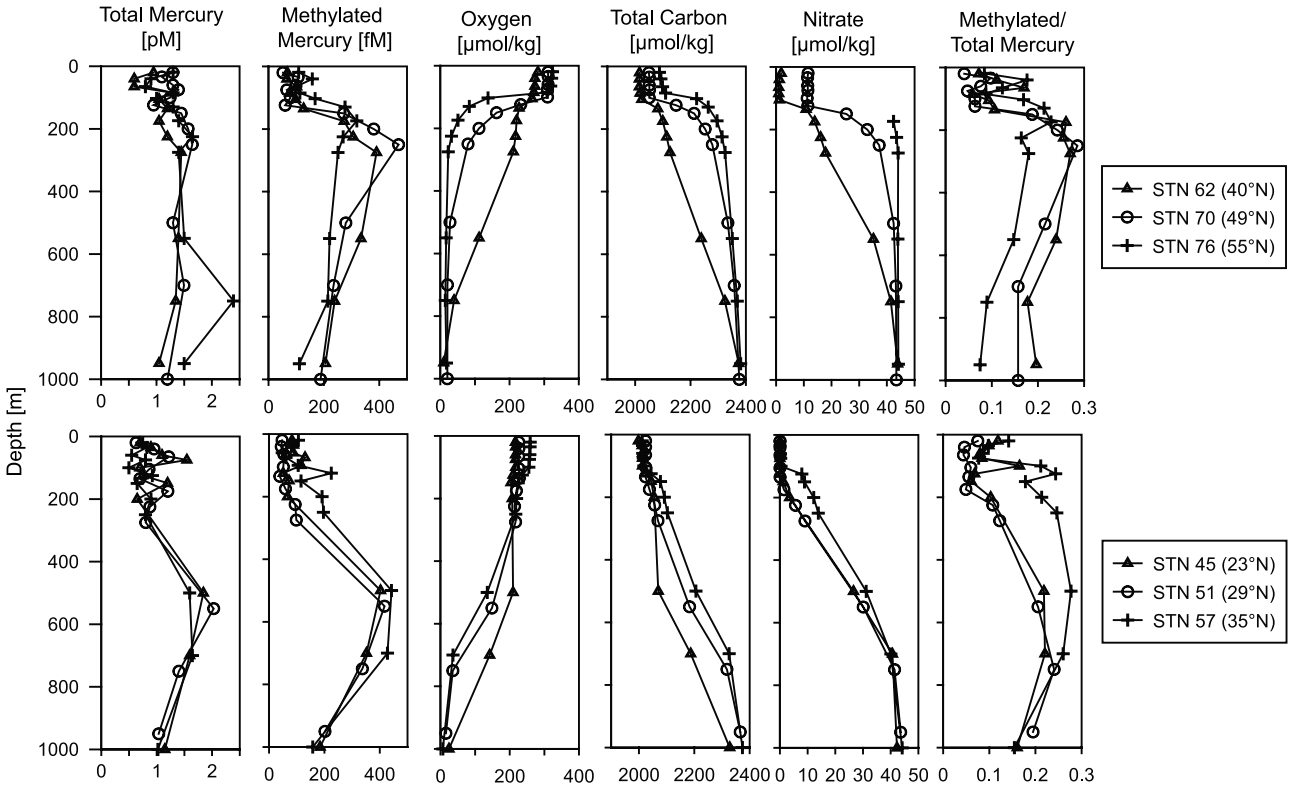

Figure 2. Vertical profiles of total Hg, methylated Hg (MeHg + Me_2Hg), oxygen, total carbon, and nitrate measured on the P16N cruise from 10–30 March 2006.

circulation among basins described by *Kahana et al.* [2004] and includes Hg inputs and losses through particle settling and remineralization, lateral and vertical seawater flow, evasion, and freshwater discharges, in addition to atmospheric deposition. Here we used upper and lower 95% confidence intervals of empirically estimated Hg concentrations and fluxes described in *Sunderland and Mason* [2007] to simulate high, low and moderate scenarios for Hg concentration changes in the North Pacific Ocean.

3. Results

3.1. Total Hg

[19] Average concentrations of total and methylated Hg (MeHg + Me_2Hg) across all stations sampled are reported in Table 2. We found significantly higher total Hg concentrations in intermediate waters, likely due to Hg losses in surface waters from particle scavenging and Hg(0) evasion, which have been reported by others [*Cossa et al.*, 1992; *Gill and Fitzgerald*, 1988; *Laurier et al.*, 2003; *Mason et al.*, 1998, 2001; *Mason and Fitzgerald*, 1993]. We also observed significant latitudinal differences in total Hg concentrations (Table 2) and vertical profiles (Figure 2).

[20] Latitudinal differences in total Hg profiles reflect circulation of the three main intermediate water masses in the North Pacific Ocean. The Pacific Subarctic water (PSW) extends from the north over much of the eastern and western North Pacific [*Favorite et al.*, 1976; *Pickard and Emery*, 1990]. The PSW mixes with the North Pacific Central Water (NPCW) and the North Pacific Intermediate Water (NPIW) around 40°N [*Pickard and Emery*, 1990]. In Figure 3, the characteristically low temperatures (2–4°C) and salinities (33.5–34.5 ppt) of the PSW are clearly distinguishable from the warmer, more saline NPCW. A drop in salinity and

Table 2. Summary of Measured Hg Concentrations in the North Pacific Along the 2006 P16N Cruise Track[a]

Description	Total Hg (pM)	Methylated Hg (fM)	Percent Methylated
All samples (n = 80)	1.14 ± 0.38 (0.50–2.39)	161 ± 115 (n/d–470)	14 ± 7 (2–29)
Depth <150 m (n = 48)	0.99 ± 0.32 (0.50–1.94)	95 ± 52 (n/d–276)	10 ± 5 (2–24)
Depth >150 m (n = 32)	1.35 ± 0.37 (0.65–2.39)	260 ± 114 (59–470)	19 ± 6 (5–29)
Difference between depths	* (p < 0.001)	* (p < 0.001)	* (p < 0.001)
Latitude <40°N (n = 34)	1.02 ± 0.39 (0.50–2.03)	154 ± 125 (n/d–442)	14 ± 7 (4–28)
Latitude >40°N (n = 36)	1.26 ± 0.32 (0.60–2.39)	191 ± 110 (52–470)	15 ± 7 (4–29)
Difference between latitudes	* p < 0.05	n/s	n/s

[a]Data are shown as sample means and standard deviations by depth and latitude with minimum and maximum values shown in brackets. Not significant, n/s; below detection limits, n/d; asterisk denotes significant difference using a t test for two samples with unequal variances.

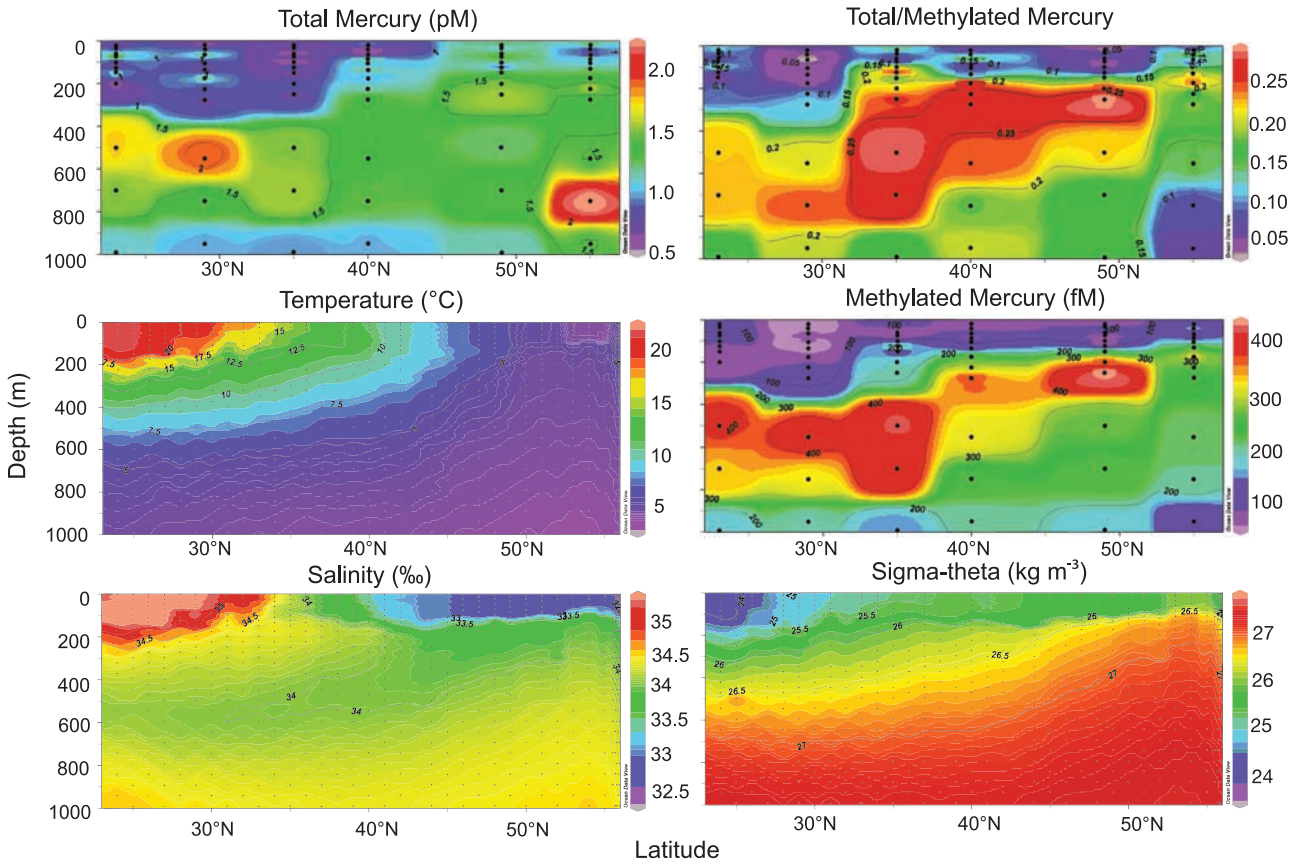

Figure 3. Interpolated cross-sectional latitudinal surfaces along the P16N cruise track at 152°W in the eastern North Pacific for Hg and other hydrographic properties. Observational data are shown as black dots.

temperature between depths of ~300–700 m (Figure 3) in subsurface waters below the NPCW indicates the presence of the NPIW [*Talley*, 1993]. Both the NPCW and NPIW originate in the western North Pacific and are transported eastward in a clockwise circulation gyre [*Pickard and Emery*, 1990; *Ueno and Yasuda*, 2003]. Data on the PSW suggest that these waters also outcrop in northern regions of the western North Pacific [*Ueno and Yasuda*, 2003; *Ueno et al.*, 2007]. The more homogeneous nature of the PSW compared to the NPCW and NPIW is apparent in the vertical Hg profiles collected at more northern latitudes and likely results in the observed increase in average concentrations above 40°N (Table 2).

3.2. Methylated Hg

[21] Methylated Hg concentrations are also significantly enriched in subsurface waters (*t* test for paired means, $p < 0.001$) compared to the well-mixed surface layer (Table 2). These results are consistent with the hypothesis that net production of methylated species occurs primarily in deeper, low-oxygen, thermocline waters and concentrations are replenished at the surface primarily through upwelling and diffusive transport [*Mason and Sullivan*, 1999; *Mason and Fitzgerald*, 1993]. Although both methylated Hg species break down in the presence of light, other studies have shown that Me_2Hg degradation is much more rapid than that of MeHg [*Mason and Sullivan*, 1999]. Accordingly, Me_2Hg concentrations reported in other studies are generally at or below detection limits in the euphotic zone of marine waters [*Cossa et al.*, 1997; *Horvat et al.*, 2003; *Kim and Fitzgerald*, 1986; *Kotnik et al.*, 2007; *Mason et al.*, 1998; *Mason and Sullivan*, 1999; *Mason and Fitzgerald*, 1990, 1993]. We therefore posit that methylated Hg concentrations in surface waters reported here are primarily MeHg (Table 2).

[22] We found methylated Hg makes up an average of 10 ± 5% of the total Hg in surface waters (<150 m) compared to 19 ± 6% in intermediate waters (150–1000 m) (Table 2). Profile averages of methylated Hg concentrations reported here are within the range of values found in the equatorial Pacific, higher than Atlantic Ocean measurements, and lower than those observed in the Mediterranean Sea (Table 3). We found no significant latitudinal differences in methylated Hg concentrations along the P16N cruise track, indicating related processes are likely responsible for production and distribution across all stations sampled (Table 2). However, maximal methylated Hg concentrations occur at shallower depths in the PSW, coincident with an upward trend in the oxycline and pycnocline (Figures 2–3).

[23] Vertical profiles of methylated Hg show concurrent peaks with total carbon and nitrate (Figure 2). Regions

Table 3. Methylated Hg Measurements in Various Ocean Basins[a]

Location	Methylated Hg (fM)	Percent Methylated	Reference(s)
North Pacific	173 ± 118 (n/d-470)[b]	15 ± 7	This study
Equatorial Pacific	<50–500[c]; <10–670[d]	2–15	*Mason and Fitzgerald* [1990, 1993]
North Atlantic	n/d[c]; 81 ± 68[d]	n/d–7	*Mason et al.* [1998]
South and equatorial Atlantic	25–200[c]; <10–110[d]	5–10	*Mason and Sullivan* [1999]
Mediterranean Sea	280 ± 120[c]; 3 ± 3[d]	25 ± 10	*Kotnik et al.* [2007]
	290 ± 26[c]; 3 ± 2[d]	19 ± 5	*Horvat et al.* [2003]
	<150[c]; <20–290[d]		*Cossa et al.* [1997]

[a]Below detection limits: n/d.
[b]Methyled Hg concentrations averaged across six vertical profiles (n = 64).
[c]Methylmercury (MeHg).
[d]Dimethylmercury (Me_2Hg).

with maximal total carbon and nutrient concentrations exhibit corresponding low oxygen concentrations, suggesting organic matter decomposition (Figure 2). Accordingly, we found a significant negative correlation between dissolved oxygen and methylated Hg concentrations in this study (Spearman rank correlation coefficient: $r_s = -0.60$; $p < 0.001$), which supports our proposed link between organic carbon remineralization, dissolved oxygen suppression, and production of methylated Hg. *Kirk et al.* [2008] also found a significant negative correlation between water column MeHg and dissolved oxygen in the Arctic Ocean/Hudson Bay.

4. Discussion

4.1. Methylated Hg Production and Distribution

[24] Ambient methylated Hg concentrations in aquatic systems reflect the supply of bioavailable Hg(II), activity of methylating microbes, and relative rates of demethylation [*Benoit et al.*, 2003]. Previous oceanic research supports relationships among methylated Hg production, biological productivity, sinking of particulate organic carbon (POC), and microbial activity associated with organic carbon remineralization [*Cossa et al.*, 1992; *Mason and Fitzgerald*, 1993; *Mason et al.*, 1998; *Mason and Sullivan*, 1999; *Mason et al.*, 2001; *Monperrus et al.*, 2007a]. Here we hypothesize that POC transport and remineralization is intrinsically linked to the production and distribution of methylated Hg species by providing a source of Hg(II) to microbially active subsurface waters and by stimulating heterotrophic activity. In addition, we posit that methylated Hg production is indirectly related to primary productivity through the POC export flux.

4.1.1. Supply of Hg(II) to Subsurface Waters

[25] In the euphotic zone of marine waters, growing phytoplankton populations take up inorganic carbon and nutrients and produce oxygen and particulate organic carbon (POC). When these plankton die, a fraction of the POC produced sinks into deeper waters (better known as the export flux or particle rain) [*Feely et al.*, 2004; *Schlitzer*, 2004]. Inorganic Hg(II) is strongly sorbed by organic matter in the water column and transported to deeper waters with sinking POC [*Mason and Fitzgerald*, 1993; *Mason and Lawrence*, 1999]. Remineralization of sinking POC by heterotrophic bacteria in subsurface waters results in consumption of oxygen and releases carbon, nutrients, and sorbed Hg(II) back to the water column [*Feely et al.*, 2004; *Mason et al.*, 1998]. Thus, POC export can remove Hg(II) from surface waters and provides a source of potentially bioavailable Hg(II) in intermediate waters during organic carbon decomposition.

[26] We modeled particulate export of Hg in the North Pacific on the basis of reported primary productivity, carbon flux curves developed by *Antia et al.* [2001], and using the parameterization for Hg described in *Sunderland and Mason* [2007]. The resulting annual flux of Hg(II) is 0.90 Mmol (6.59 μg m^{-2} a^{-1}) at 100 m depth and 0.40 Mmol (2.93 μg m^{-2} a^{-1}) at 300 m depth, giving an annual Hg(II) dissolution of 0.50 Mmol (91 fM a^{-1}) between depths of 100 and 300 m and 0.22 Mmol (6.7 fM a^{-1}) between 300 and 1500 m during organic carbon remineralization. Comparatively, annual Hg inputs to the North Pacific Ocean (>30°N) from atmospheric deposition are 2.1 Mmol (basin-wide average 15.4 μg m^{-2} a^{-1}) [*Selin et al.*, 2008] and 0.55 Mmol from rivers (77% derived from the Asian continent) [*Sunderland and Mason*, 2007]. These modeling results support the supposition that biological productivity and resulting POC transport supplies substantial amounts of inorganic Hg to subsurface waters in the North Pacific Ocean, particularly immediately below the euphotic zone. In deeper waters (>500 m), transport of Hg(II) with lateral circulation of the NPIW and other water masses may be more important, as discussed in section 4.2.

4.1.2. Effects of POC Remineralization on Hg Methylation

[27] We found a phenomenological ''hump-shaped'' (second-order polynomial) relationship between methylated Hg concentrations, the distribution of remineralized carbon (C_{rm}), and apparent oxygen utilization (*AOU*) in intermediate waters from the eastern North Pacific (Figure 4). Concentrations of remineralized carbon (C_{rm}) and *AOU* in intermediate waters can be strongly affected by circulation of water masses in addition to changes resulting from remineralization of vertically settling POC [*Najjar et al.*, 2007]. Elevated values for *AOU* and C_{rm} shown in Figure 4 therefore may not reflect potential methylated Hg species production associated with active POC remineralization processes. Accordingly, by correcting for the effects of circulation using water mass ages, we found a significant linear relationship ($r^2 = 0.66$, $p < 0.001$) between increasing rates of organic carbon remineralization (*OCRR*) and enhanced methylated Hg concentrations (Figure 4). This means that when POC decomposition rates are low, ambient methylated Hg concentration are also low. Maximal methylated Hg concentrations correspond to

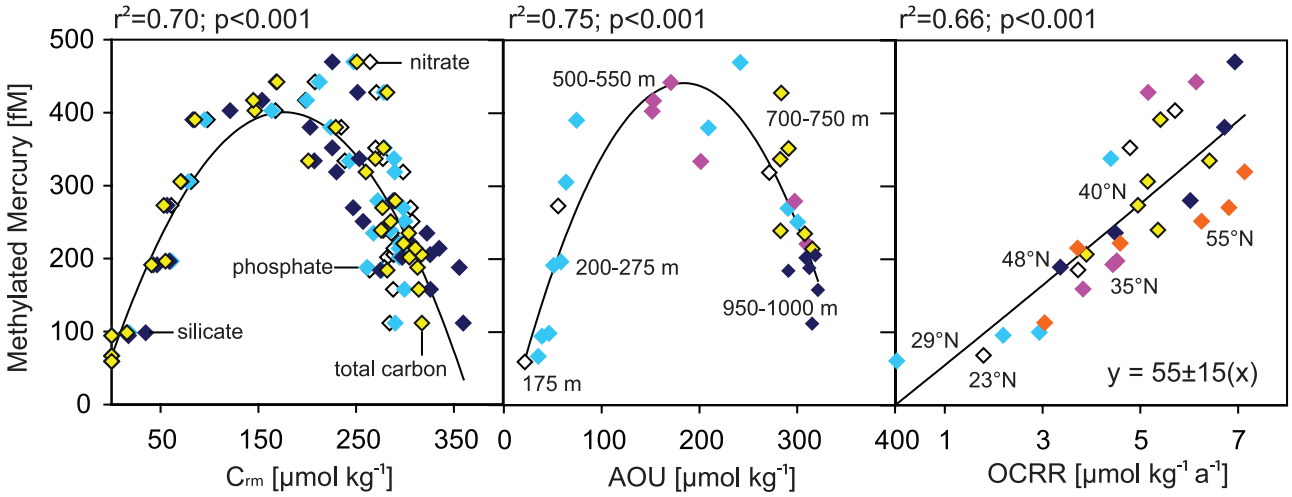

Figure 4. Observed relationships between methylated Hg (MeHg + Me_2Hg) concentrations in intermediate waters (150–1000 m depth) and several proxies for organic matter decomposition and heterotrophic activity. C_{rm} = the distribution of remineralized carbon calculated from measured total carbon, nitrate, phosphate and silicate concentrations; AOU, Apparent Oxygen Utilization; OCRR, Organic Carbon Remineralization Rates. Note that additional data points for the C_{rm} plot reflects the use of four different predictors of methylated Hg concentrations. In addition, some values of OCRR could not be calculated for deeper waters because measured pCFC-12 data were not available, reducing the total sample size shown.

the highest *OCRR*s (Figure 4) as well as the location of the oxycline across all stations (Figure 2), which reflects consumption of oxygen during POC remineralization.

[28] These results are consistent with our original hypothesis that POC transport and remineralization processes are extremely important for the production and distribution of methylated Hg species. In addition to providing a source of Hg(II) to subsurface waters, settling POC decomposition may stimulate Hg methylation by providing a substrate for bacterial activity. Remineralization of POC also creates a geochemical gradient in the water column between high levels of dissolved oxygen and more reducing conditions. For example, export of POC from productive surface waters above the PSW results in severely oxygen-depleted conditions in subsurface waters (Figures 2–3). Such geochemical conditions are conducive to the activity of microbial functional groups (e.g., sulfate- and iron-reducing bacteria) known to be capable of methylation from research in other environments [*Benoit et al.*, 2003; *Fleming et al.*, 2006; *Hammerschmidt and Fitzgerald*, 2004; *Heyes et al.*, 2006; *Kerin et al.*, 2006; *Sunderland et al.*, 2004]. For example, *Sunderland et al.* [2004] found methylation in estuarine sediments is enhanced by the presence of organic carbon "pockets" that create microzonal redox gradients in the sediment stratigraphy. Similarly, it is plausible that water column MeHg production in pelagic marine waters can occur inside fecal pellets and marine snow aggregates, since they have very low internal oxygen levels. Elevated levels of dissolved reduced Fe(II) were measured in all of the P16N profiles below 500 m (W. M. Landing, unpublished data, 2008). Because the pE/pH conditions are not appropriate for thermochemical dissolved Fe(III) reduction in the water column, we attribute the elevated Fe(II) concentrations to reduction in reducing microenvironments (inside pellets and aggregates), and release to the water column coupled with slow reoxidation kinetics in cold, low-pH, low-oxygen waters below 500 m. Thus, the observed relationship between *OCRR* and MeHg and our proposed methylation mechanism for the North Pacific Ocean does not require Hg(II) attached to settling POC to be released to the water column prior to being taken up by bacteria for methylation (i.e., direct incorporation of particulate-associated Hg during organic carbon remineralization is plausible).

[29] Our results showing relatively low methylated Hg concentrations in both surface waters and older, deeper waters between 700 and 1000 m depths with high *AOU* and C_{rm} (Figure 4) suggest that net production of MeHg and Me_2Hg is not occurring throughout the entire water column. Both MeHg and Me_2Hg are unstable in seawater and therefore require constant production for accumulation to occur [*Mason and Sullivan*, 1999; *Whalin et al.*, 2007]. Decomposition of methylated Hg is enhanced by light but also takes place (at a relatively slower rate) in deeper waters [*Mason and Sullivan*, 1999]. In addition, MeHg is particle reactive (although Me_2Hg is not) and can be gradually removed from the water column with settling particles [*Mason and Fitzgerald*, 1993].

[30] Concentrations of POC in subsurface waters and associated remineralization rates are indirectly related to primary productivity through the export flux [*Schlitzer*, 2004]. This explains why other studies have observed relationships between productivity in surface waters and methylated Hg concentrations. For example, *Mason et al.* [1998] cited data showing elevated Me_2Hg levels in subsurface waters underlying highly productive equatorial Pacific waters, compared to those in relatively low productivity

regions in the North Atlantic and western Pacific Oceans. Similarly, *Monperrus et al.* [2007a] found water column methylation rates in the Mediterranean Sea are proportional to the abundance and activity of pelagic microorganisms (phyto- and bacterioplankton).

4.1.3. Importance of Water Column Methylation Processes

[31] Although some studies propose that lateral transport along isopycnal surfaces and diffusion from deep sediments could account for the majority of MeHg in marine waters [*Hammerschmidt and Fitzgerald*, 2006b; *Kraepiel et al.*, 2003], our findings are more consistent with recent data from the Mediterranean and Hudson Bay region of the Canadian Arctic, showing active water column production [*Kirk et al.*, 2008; *Monperrus et al.*, 2007a]. *Monperrus et al.* [2007a] measured rates of in situ water column production of MeHg and Me_2Hg using isotopically labeled Hg(II) and, similar to *Kirk et al.* [2008], proposed that such production accounts for the majority of methylated species. In addition, *Blum et al.* [2008] recently used natural Hg isotope abundance ratios to show that MeHg in pelagic marine fish such as tuna likely originates from open ocean Hg methylation processes.

[32] Further research is needed to investigate the relationship between production of methylated Hg species, POC transport and heterotrophic activity in open ocean environments. However, the relationships presented here provide a starting point for assessing variability in methylated Hg species distribution in different ocean basins using readily available global databases for oxygen, total carbon and nutrients to calculate *OCRR*.

4.2. Temporal Trends in Hg Concentrations

[33] After comparing profile data for total Hg from several cruises spanning a 20-year period, *Laurier et al.* [2004] concluded that there has been no change in North Pacific Hg concentrations over the last several decades. Surface water concentrations (>20 m depth) observed in this study (2006), show no apparent change in concentrations relative to observations at similar latitudes in 2002 and 1987 (Figure 5). In contrast, the average total Hg concentration across all stations for the P16N cruise in 2006 (1.14 ± 0.38 pM) is significantly higher than the Intergovernmental Oceanographic Commission (IOC) cruise in 2002 (0.64 ± 0.26 pM) and the Vertical Transport and Exchange Survey (VERTEX) cruise in 1987 (0.58 ± 0.37 pM) (t test for paired means, $p < 0.05$). Similarly, comparing average profile concentrations (surface to 1000 m depth) across all stations sampled in this study to those from previous studies at the same latitudes in the North Pacific shows enriched concentrations in intermediate waters at all locations (Figure 6). *Laurier et al.* [2004] found that North Pacific Hg concentrations in the upper 500 m of the water column vary seasonally with peak concentrations observed during summer months and lowest levels during the winter. Since both the IOC and P16N cruises took place in the spring months (March–May), profile comparisons with the VERTEX cruise (July–August 1987) shown here (Figure 6) may underestimate temporal changes in seawater concentrations.

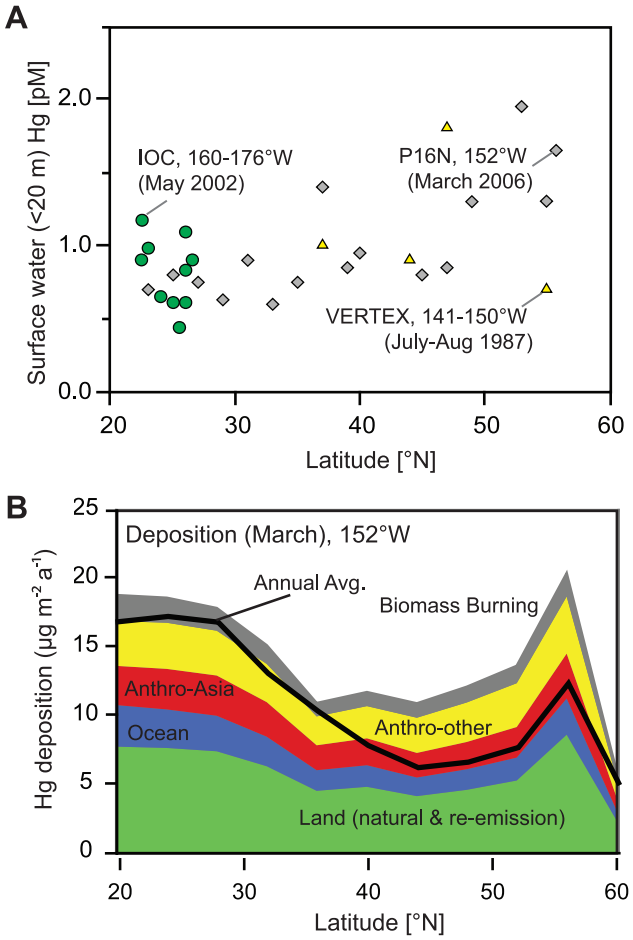

Figure 5. (a) Surface water (<20 m depth) Hg concentrations from P16N cruise compared to previous cruise data in the eastern North Pacific. Other data shown are from the IOC (International Oceanographic Commission Baseline Trace Metal) cruise between 1 May 2002 and 4 June 2002 and the Vertical Transport and Exchange (VERTEX) research cruise in 1987 described by *Laurier et al.* [2004]. (b) Modeled source attribution of atmospheric deposition along the P16N cruise track using the GEOS-Chem global atmospheric chemistry model [*Strode et al.*, 2008].

4.2.1. Surface Waters (<20 m) and Atmospheric Deposition

[34] Mercury concentrations in the well-mixed surface layer are more likely to reflect recent trends in atmosphere deposition than intermediate waters because the time required for mixing and equilibration with atmospheric Hg inputs is generally less than 1 year [*Lamborg et al.*, 2002; *Selin et al.*, 2008; *Strode et al.*, 2007]. We compared modeled atmospheric deposition along the P16N cruise track to latitudinal trends in surface (<20 m) seawater concentrations (Figure 5). Source attribution of atmospheric deposition reveals that although rates vary from ~6–20 $\mu g\ m^{-2}\ a^{-1}$ across the cruise track, the relative contributions to deposition from various sources remain similar (Figure 5b). For example, global anthropogenic emissions account for approximately one third (32–37%) of

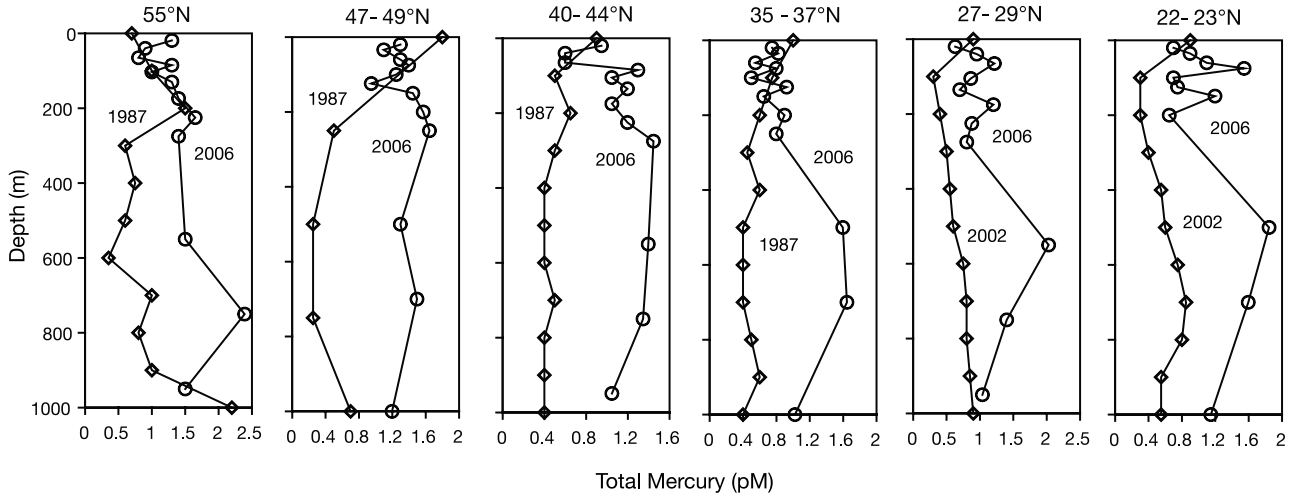

Figure 6. Comparison of total Hg profiles from the P16N cruise in March 2006, the IOC cruise in May–June 2002, and the VERTEX cruise in July–August 1987. Note that seasonal enrichment of water column Hg during the summer months compared to the spring months means that differences in Hg concentrations between the VERTEX and IOC/P16N cruises are likely greater than indicated by the samples shown here.

total deposition along the P16N cruise track, while biomass burning combined with natural and reemitted Hg emissions from terrestrial and oceanic systems account for the remaining two thirds. These results are consistent with Hg(0) oxidation and deposition from the well-mixed global atmospheric pool in the eastern North Pacific, rather than a dominant source region [*Selin et al.*, 2007; *Strode et al.*, 2008].

[35] Asian anthropogenic emissions have risen steadily over the past several decades and presently comprise more than 50% of the global anthropogenic source [*Pacyna et al.*, 2006]. However, since Asian anthropogenic sources constitute between 15 and 18% of total deposition along the P16N cruise track (Figure 5b), even doubling Asian emissions would likely increase deposition rates by less than 20%, assuming similar speciation. In addition, if such increases in atmospheric deposition were reflected proportionally in seawater in the eastern North Pacific, changes would still be difficult to discern from high levels of spatial and seasonal variability noted in other studies [*Laurier et al.*, 2004].

[36] Overall, these results suggest variability in atmospheric deposition rates along the P16N cruise track mainly reflects meteorological and chemical factors determining oxidation of atmospheric Hg(0) and subsequent transport and deposition of Hg(II). For example, the most pronounced similarity between surface water concentrations and deposition along the P16N cruise track occurs as a concurrent peak just above 50°N (Figure 5). This peak corresponds to the location of a semipermanent low-pressure area with high rates of convective transport known as the Aleutian low region, which likely results in enhanced atmospheric transport and downwelling of Hg from the upper troposphere [*Selin and Jacob*, 2008; *Selin et al.*, 2007; *Strode et al.*, 2008].

[37] In contrast to results for the eastern North Pacific reported here, enriched Hg concentrations in western North Pacific surface waters (Figure 7) match areas of enhanced atmospheric deposition shown in *Strode et al.* [2008]. Increased atmospheric deposition rates in the western North Pacific off the coast of Japan reflect the localized signal of Hg(II) emissions from Asian sources rather than oxidation and deposition of Hg(0) from the well-mixed global pool [*Jaffe and Strode*, 2008; *Strode et al.*, 2008]. Throughout this region, contributions to deposition from Asian sources are a minimum of twofold greater than in the eastern North Pacific (>45%) [*Strode et al.*, 2008].

[38] Intermediate waters that travel in a clockwise direction to the eastern North Pacific originate in the western North Pacific [*Pickard and Emery*, 1990]. A variety of studies have shown that the NPIW is formed when surface waters at the convergence between the Oyashio and Kuroshio currents sink and are mixed with deeper waters [*Talley*, 1993; *Ueno and Yasuda*, 2003; *Ueno et al.*, 2007]. The NPIW then travels eastward along the same trajectory as the North Pacific current shown in Figure 7. Because there is no evidence for a recent change in atmospheric Hg deposition and surface water concentrations in the eastern North Pacific, as discussed above, Hg enriched waters off the coast of Japan that become part of the NPIW are a probable source for the observed increase in intermediate water concentrations (Figure 6).

4.2.2. Enrichment of Intermediate Water Masses

[39] Mercury concentrations in intermediate waters reflect a combination of processes including inputs and losses at the air-sea interface, diffusion, lateral flow, and particle-associated transport [*Mason and Sullivan*, 1999; *Mason and Fitzgerald*, 1993; *Sunderland and Mason*, 2007]. Intermediate waters may also exhibit a substantial lag before changes in atmospheric inputs are fully reflected in ambient seawater concentrations [*Sunderland and Mason*, 2007]. With the exception of a single outlier above 55°N, Hg concentrations reported here peak in the NPIW (Figure 2).

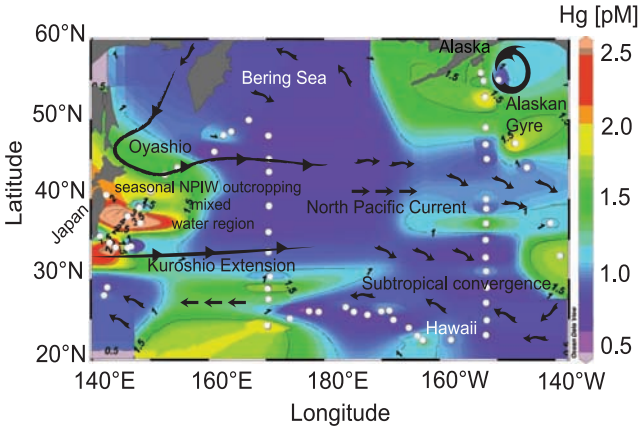

Figure 7. Surface water Hg concentration data (<20 m depth) interpolated from all previous cruises on the North Pacific Ocean. Surface circulation was adapted from *Pickard and Emery* [1990]. Observational data are shown as white dots.

These results support the hypothesis that lateral transport of Hg enriched waters from the western North Pacific are important determinants of intermediate water concentrations in the eastern North Pacific. It therefore follows that the relative Hg enrichment in intermediate waters observed here compared to earlier cruise data (IOC-2002 and VERTEX-1987) are attributable to similar processes (Figures 6). More specifically, a rise in Asian anthropogenic emissions, deposition and Hg concentrations in coastal waters has resulted in enhanced Hg concentrations in intermediate waters that are now detectable in the eastern North Pacific (Figures 6 and 8a).

[40] We performed simple calculations using average zonal velocities (Lowered Acoustic Doppler Current Profiler (LADCP) measurements during the P16N cruise) of subsurface waters to test whether horizontal transport could feasibly explain the observed temporal trends in Hg concentrations. Rates of subsurface eastward flow generally ranged between 5 and 10 cm s^{-1} [*Feely et al.*, 2006]. If we assume a net eastward transport of 5 cm s^{-1} in intermediate water masses and approximate the distance from the coast of Japan at ~40°N to the P16N cruise track at 152°W (~650 km), about 4 years are required for newly formed waters in the NPIW mass to reach the eastern North Pacific. Although Hg enriched surface waters that become part of the NPIW are diluted by mixing with deeper waters, thereby lowering the apparent ages of the various water masses, these results suggest that the observed increase in total Hg concentrations between the IOC (2002) and the P16N (2006) cruises may be attributable to recent rises in Asian anthropogenic sources and subsequent deposition in the western North Pacific Ocean [*Jaffe and Strode*, 2008; *Pacyna et al.*, 2006; *Strode et al.*, 2008].

4.2.3. Modeled Changes in Intermediate Waters

[41] Similarly, modeled trajectories of basin-wide Hg concentrations using the *Sunderland and Mason* [2007] model suggest a relatively rapid near-term increase in intermediate waters of the North Pacific at present atmospheric Hg deposition rates (Figure 8b). Although data for model evaluation are limited, the concentration trajectory shown in Figure 8b also agrees with observed increases between the P16N cruise and VERTEX/IOC campaigns. Modeling results suggest basin-wide Hg concentrations in

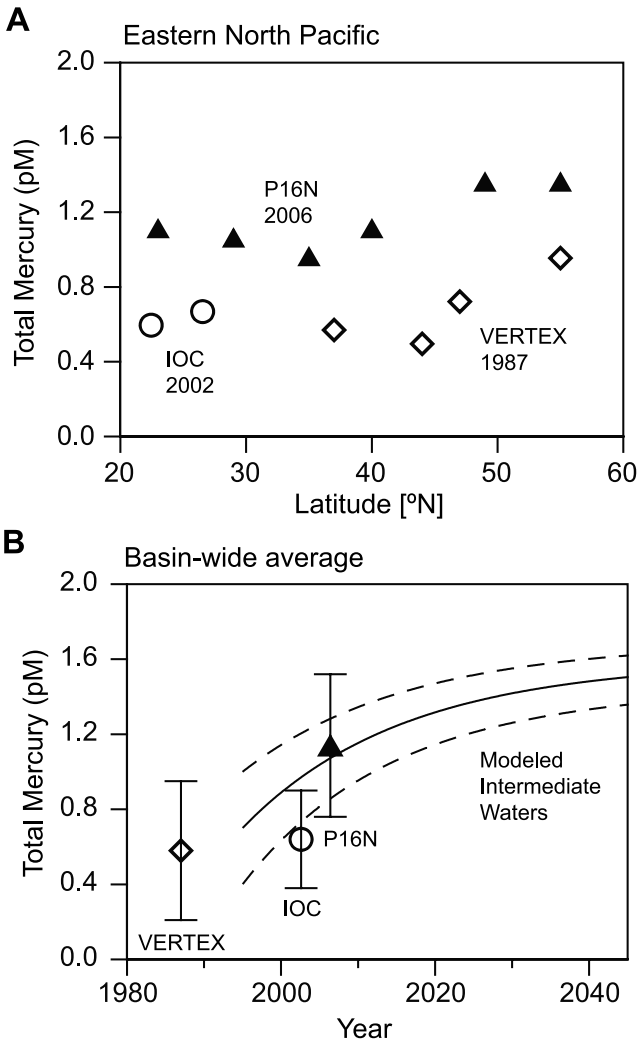

Figure 8. (a) Average total Hg concentrations in integrated 1000 m profiles from the eastern North Pacific. Data are from the P16N cruise from 10–30 March 2006, the IOC cruise from 1 May to 4 June 2002 and the VERTEX cruise between July and August 1987 [*Laurier et al.*, 2004]. (b) Modeled temporal trends in basin wide Hg concentrations in the North Pacific Ocean with no change in contemporary atmospheric Hg deposition. Dashed lines represent 95% confidence intervals for modeling results. Overall averages of vertical profiles between 0 and 1000 m depths from the P16N (2006), IOC (2002), and VERTEX (cruises) are also shown, with error bars equivalent to one standard deviation from the mean measured concentration. Annually averaged differences between cruises in 1987 and 2002/2006 are likely underestimated by the values shown because of enrichment in water column Hg known to occur in the summer months during the VERTEX (1987) sampling period compared to spring samples collected on both the IOC and P16N cruises.

North Pacific intermediate waters increased at an average rate of 3% per year between 1995 and 2006 (Figure 8b). If contemporary atmospheric deposition rates are maintained, intermediate waters may experience a doubling of Hg concentrations (compared to ca. 1995) by 2050 (Figure 8b).

5. Summary and Conclusions

[42] We observed maximal concentrations of methylated Hg species in the eastern North Pacific in subsurface, low-oxygen, thermocline waters known to have high levels of bacterial activity (Figure 2). In addition, we found a positive linear relationship between increasing rates of organic carbon remineralization (*OCRR*) and methylated Hg concentrations, which points to a link between organic carbon utilization and Hg methylation in the open ocean (Figure 4). The consistency of Redfield-type relationships throughout the intermediate water masses suggests the majority of organic carbon decomposition is from relatively intact rapidly settling particles rather than partially decomposed organic material advected from other areas. These results agree with our hypothesis that POC transport and remineralization exerts a dominant control over the production and distribution of methylated Hg species by providing a source of Hg(II) to microbially active subsurface waters and by stimulating heterotrophic bacterial activity. Methylated Hg production and accumulation is therefore indirectly related to biological productivity through the POC export flux.

[43] Degradation and export processes for MeHg and Me_2Hg contribute to lower relative methylated Hg concentrations in older, deeper waters with high *AOU* and C_{rm}. Relationships among water column methylated Hg concentrations, *AOU*, C_{rm} and *OCRR* presented here are based on widely available ocean cruise data such as carbon, oxygen, and nutrients and therefore provide a starting point for characterizing the distribution of methylated Hg species in open ocean environments.

[44] Our results also show that total Hg concentrations in intermediate waters are elevated relative to earlier cruises (Figures 6 and 8). Elevated Hg concentrations in waters off the coast of Japan that are laterally transported in intermediate water masses to the eastern North Pacific are a probable source for this enrichment (Figure 7). Thus, the near-term rise in Asian anthropogenic emissions and deposition in coastal waters of the western Pacific may now be affecting basin-wide Hg levels of the North Pacific Ocean. Supporting this premise, modeled trajectories suggest a relatively rapid near term increase in basin-wide Hg concentrations over the next several decades if contemporary atmospheric deposition rates are maintained (Figure 8). Such increases could have serious implications for resulting contaminant burdens in pelagic marine fish if methylated Hg species production mimics total Hg concentration trends.

[45] **Acknowledgments.** Financial support for this study was provided by the USGS Toxic Substances Hydrology Program and the Chemical Oceanography Program of the National Science Foundation (W. M. Landing, OCE-0223378 and OCE-0649639). The authors acknowledge the NSF/NOAA-funded U.S. Repeat Hydrography Program and the NOAA Climate Program. Data used in this manuscript were provided by the following participants in the Leg 2 CLIVAR P16N Cruise: Andreas Thurnherr (LADCP data), Richard Feely and Chris Sabine (carbon data), Gregory Johnson and Molly Baringer (bottle hydrographic measurement program), Chris Langdon (dissolved oxygen data), Calvin Mordy and Jia-Zhong Zhang (nutrient data), and Mark Warner and Wendi Ruef (CFC data). We thank Chris Holmes and Daniel Jacob at Harvard University, Noelle Selin at MIT, and Robert Mason at the University of Connecticut for useful discussion related to this manuscript. Finally, we gratefully acknowledge analytical support from John De Wild, Tom Sabin, and Shane Olund in the USGS Mercury Research Laboratory. Any use of trade, product, or firm names in this publication is for descriptive purposes only and does not imply endorsement by the U.S. Government.

References

Anderson, L. A., and J. L. Sarmiento (1994), Redfield ratios of remineralization determined by nutrient data analysis, *Global Biogeochem. Cycles*, *8*(1), 65–80, doi:10.1029/93GB03318.

Antia, A. N., et al. (2001), Basin-wide particulate organic carbon flux in the Atlantic Ocean: Regional export patterns and potential for CO_2 sequestration, *Global Biogeochem. Cycles*, *15*(4), 845–862.

Benoit, J. M., C. C. Gilmour, A. Heyes, R. P. Mason, and C. Miller (2003), Geochemical and biological controls over methylmercury production and degradation in aquatic systems, *ACS Symp. Ser.*, *835*, 262–297.

Blum, J., D. Senn, E. Chesney, and J. Shine (2008), Mercury isotope evidence for contrasting mercury sources to coastal versus offshore marine fish, paper presented at the Geological Society of America Joint Annual Meeting, Houston, Tex, 5–9 October.

Cossa, D., P. Michel, J. Noel, and D. Auges (1992), Vertical profile of total mercury in relation to arsenic, cadmium and copper distributions at the eastern North Atlantic ICES reference station, *Oceanol. Acta*, *15*, 1719–1728.

Cossa, D., J.-M. Martin, K. Takayanagi, and J. Sanjuan (1997), The distribution and cycling of mercury species in the western Mediterranean, *Deep Sea Res., Part II*, *44*(3–4), 721–740, doi:10.1016/S0967-0645(96)00097-5.

De Wild, J., M. Olson, and S. Olund (2002), Determination of methylmercury by aqueous phase ethylation, followed by gas chromatographic separation with cold vapor atomic fluorescence detection, *U.S. Geol. Surv. Open File Rep. 01-445*, 19 pp.

Doney, S., and J. Bullister (1992), A chlorofluorocarbon section in the eastern North Atlantic, *Deep Sea Res.*, *39*(11/12), 1857–1883, doi:10.1016/0198-0149(92)90003-C.

Eckley, C. S., and H. Hintelmann (2006), Determination of mercury methylation potentials in the water column of lakes across Canada, *Sci. Total Environ.*, *368*, 111–125, doi:10.1016/j.scitotenv.2005.09.042.

Ekstrom, E., E. Malcolm, J. Schaefer, and F. Morel (2006), Biotic and abiotic sources of methylmercury in the ocean, paper presented at the 8th International Conference on Mercury as a Global Pollutant, Madison, Wisc., 6–11 August.

Favorite, F., A. Dodimead, and K. Nasu (1976), *Oceanography of the Subarctic Pacific Region, 1960–1971*, 187 pp., Int. North Pacific Fisheries Comm., Vancouver, B. C.

Feely, R. A., C. Sabine, R. Schlitzer, J. Bullister, S. Mecking, and D. Greeley (2004), Oxygen utilization and organic carbon remineralization in the upper water column of the Pacific Ocean, *J. Oceanogr.*, *60*, 45–52, doi:10.1023/B:JOCE.0000038317.01279.aa.

Feely, R., C. Sabine, F. Millero, R. Wanninkhof, and D. Hansell (2006), Carbon dioxide, hydrographic, and chemical data obtained during the R/V *Thomas Thompson* cruise in the Pacific Ocean on CLIVAR repeat hydrography sections P16N_2006 (Feb. 14 – Mar. 30, 2006), report, Carbon Dioxide Inf. Anal. Cent., Oak Ridge Natl. Lab., Oak Ridge, Tenn.

Fleming, E., E. Mack, P. Green, and D. Nelson (2006), Mercury methylation from unexpected sources: Molybdate-inhibited freshwater sediments and an iron-redung bacterium, *Appl. Environ. Microbiol.*, *72*(1), 457–464, doi:10.1128/AEM.72.1.457-464.2006.

Garcia, H., and L. Gordon (1992), Oxygen solubility in seawater: Better fitting equations, *Limnol. Oceanogr.*, *37*(6), 1307–1312.

Gill, G. A., and W. F. Fitzgerald (1987), Picomolar mercury measurements in seawater using stannous chloride reduction and two-stage gold amalgamation with gas phase detection, *Mar. Chem.*, *20*, 227–243.

Gill, G., and W. F. Fitzgerald (1988), Vertical mercury distributions in the oceans, *Geochim. Cosmochim. Acta*, *52*, 1719–1728, doi:10.1016/0016-7037(88)90240-2.

Hammerschmidt, C. R., and W. F. Fitzgerald (2004), Geochemical controls on the production and distribution of methylmercury in near-shore marine sediments, *Environ. Sci. Technol.*, *38*(5), 1487–1495, doi:10.1021/es034528q.

Hammerschmidt, C. R., and W. F. Fitzgerald (2006a), Bioaccumulation and trophic transfer of methylmercury in Long Island Sound, *Arch. Environ. Contam. Toxicol.*, *51*, 416–424, doi:10.1007/s00244-005-0265-7.

Hammerschmidt, C. R., and W. F. Fitzgerald (2006b), Methylmercury cycling in sediments on the continental shelf of southern New England, *Geochim. Cosmochim. Acta*, *70*(4), 918–930, doi:10.1016/j.gca.2005.10.020.

Heyes, A., R. P. Mason, E.-H. Kim, and E. Sunderland (2006), Mercury methylation in estuaries: Insights from measuring rates using stable mercury isotopes, *Mar. Chem.*, *102*, 134–147, doi:10.1016/j.marchem.2005.09.018.

Hintelmann, H., and R. D. Evans (1997), Application of stable isotopes in environmental tracer studies: Measurement of monomethylmercury by isotope dilution ICP-MS and detection of species transformation, *Fresenius J. Anal. Chem.*, *358*, 378–385, doi:10.1007/s002160050433.

Horvat, M., L. Liang, and N. S. Bloom (1993), Comparison of distillation with other current isolation methods for the determination of methyl mercury compounds in low level environmental samples, *Anal. Chim. Acta*, *282*(1992), 153–168.

Horvat, M., J. Kotnik, M. Logar, V. Fajon, T. Zvonaric, and N. Pirrone (2003), Speciation of mercury in surface and deep-sea waters in the Mediterranean Sea, *Atmos. Environ.*, *37*(S1), 93–108, doi:10.1016/S1352-2310(03)00249-8.

Jaffe, D., and S. Strode (2008), Sources, fate and transport of atmospheric mercury from Asia, *Environ. Chem.*, *5*(2), 121–126, doi:10.1071/EN08010.

Kahana, R., G. R. Bigg, and M. R. Wadley (2004), Global ocean circulation modes derived from a multiple box model, *J. Phys. Oceanogr.*, *34*, 1811–1823, doi:10.1175/1520-0485(2004)034<1811:GOCMDF>2.0.CO;2.

Kerin, E., C. C. Gilmour, E. Roden, M. Suzuki, J. Coates, and R. P. Mason (2006), Mercury methylation by dissimilatory iron-reducing bacteria, *Appl. Environ. Microbiol.*, *72*(12), 7919–7921, doi:10.1128/AEM.01602-06.

Kim, J., and W. F. Fitzgerald (1986), Sea-air partitioning of mercury in the equatorial Pacific Ocean, *Science*, *231*(4742), 1131–1133, doi:10.1126/science.231.4742.1131.

Kirk, J. L., V. St. Louis, H. Hintelmann, I. Lehnherr, B. Else, and L. Poissant (2008), Methylated mercury species in marine waters of the Canadian High and Sub Arctic, *Environ. Sci. Technol.*, *42*(22), 8367–8373, doi:10.1021/es801635m.

Kotnik, J., et al. (2007), Mercury speciation in surface and deep waters of the Mediterranean Sea, *Mar. Chem.*, *107*, 13–30, doi:10.1016/j.marchem.2007.02.012.

Kraepiel, A., K. Keller, H. Chin, E. Malcolm, and F. Morel (2003), Sources and variations of mercury in tuna, *Environ. Sci. Technol.*, *37*, 5551–5558, doi:10.1021/es0340679.

Lamborg, C., W. F. Fitzgerald, J. O'Donnell, and T. Torgensen (2002), A non-steady-state compartmental model of global scale mercury biogeochemistry with interhemispheric atmospheric gradients, *Geochim. Cosmochim. Acta*, *66*(7), 1105–1118, doi:10.1016/S0016-7037(01)00841-9.

Laurier, F., R. P. Mason, L. Whalin, and S. Kato (2003), Reactive gaseous mercury formation in the North Pacific Ocean's marine boundary layer: A potential role of halogen chemistry, *J. Geophys. Res.*, *108*(D17), 4529, doi:10.1029/2003JD003625.

Laurier, F., R. P. Mason, G. Gill, and L. Whalin (2004), Mercury distribution in the North Pacific Ocean: 20 years of observations, *Mar. Chem.*, *90*(1–4), 3–19, doi:10.1016/j.marchem.2004.02.025.

Lee, K. (2001), Global net community production estimated from the annual cycle of surface water total dissolved organic carbon, *Limnol. Oceanogr.*, *46*, 1287–1297.

Mason, R. P., and W. F. Fitzgerald (1990), Alkylmercury species in the equatorial Pacific, *Nature*, *347*, 457–459, doi:10.1038/347457a0.

Mason, R. P., and W. F. Fitzgerald (1991), Mercury speciation in open ocean waters, *Water Air Soil Pollut.*, *56*, 779–789.

Mason, R. P., and W. F. Fitzgerald (1993), The distribution and cycling of mercury in the equatorial Pacific Ocean, *Deep Sea Res., Part I*, *40*(9), 1897–1924, doi:10.1016/0967-0637(93)90037-4.

Mason, R. P., and G. Gill (2005), Mercury in the marine environment, in *Mercury: Sources, Measurements, Cycles, and Effects*, edited by M. B. Parsons and J. B. Percival, pp. 179–216, *Short Course Ser.*, vol. 34, Mineral. Assoc. of Canada, Halifax, Nova Scotia, Canada.

Mason, R. P., and A. L. Lawrence (1999), Concentration, distribution, and bioavailability of mercury and methylmercury in sediments of Baltimore Harbor and Chesapeake Bay, Maryland, USA, *Environ. Toxicol. Chem.*, *18*(11), 2438–2447, doi:10.1897/1551-5028(1999)018<2438:CDABOM>2.3.CO;2.

Mason, R. P., and G.-R. Sheu (2002), Role of the ocean in the global mercury cycle, *Global Biogeochem. Cycles*, *16*(4), 1093, doi:10.1029/2001GB001440.

Mason, R. P., and K. A. Sullivan (1999), The distribution and speciation of mercury in the south and equatorial Atlantic, *Deep Sea Res., Part II*, *46*, 937–956, doi:10.1016/S0967-0645(99)00010-7.

Mason, R. P., K. Rolfhus, and W. F. Fitzgerald (1998), Mercury in the North Atlantic, *Mar. Chem.*, *61*, 37–53, doi:10.1016/S0304-4203(98)00006-1.

Mason, R. P., N. Lawson, and G.-R. Sheu (2001), Mercury in the Atlantic Ocean: Factors controlling air-sea exchange of mercury and its distribution in upper waters, *Deep Sea Res., Part II*, *48*, 2829–2853, doi:10.1016/S0967-0645(01)00020-0.

Measures, C., W. Landing, M. Brown, and C. Buck (2008), A commercially available rosette system for trace metal-clean sampling, *Limnol. Oceanogr. Methods*, *6*, 384–394.

Mergler, D., H. Anderson, L. Chan, K. Mahaffey, M. Murray, M. Sakamoto, and A. Stern (2007), Methylmercury exposure and health effects in humans: A worldwide concern, *Ambio*, *36*(1), 3–11, doi:10.1579/0044-7447(2007)36[3:MEAHEI]2.0.CO;2.

Millero, F. J. (2006), *Chemical Oceanography*, 3rd ed., 496 pp., CRC Press, Boca Raton, Fla.

Monperrus, M., E. Tessier, D. Amouroux, A. Leynaert, P. Huonnic, and O. Donard (2007a), Mercury methylation, demethylation and reduction rates in coastal and marine surface waters of the Mediterranean Sea, *Mar. Chem.*, *107*, 49–63, doi:10.1016/j.marchem.2007.01.018.

Monperrus, M., et al. (2007b), The biogeochemistry of mercury at the sediment-water interface in the Thau Lagoon: 2. Evaluation of mercury methylation potential in both surface sediment and the water column, *Estuarine Coastal Shelf Sci.*, *72*, 485–496, doi:10.1016/j.ecss.2006.11.014.

Najjar, R., et al. (2007), Impact of circulation on export production, dissolved organic matter, and dissolved oxygen in the ocean: Results from Phase II of the Ocean Carbon-cycle Model Intercomparison Project (OCMIP-2), *Global Biogeochem. Cycles*, *21*, GB3007, doi:10.1029/2006GB002857.

National Research Council (2000), Toxicological Effects of Methylmercury, edited by the Board on Environ. Sci. and Toxicol., 368 pp., Natl. Acad. Press, Washington, D. C.

Pacyna, E., J. Pacyna, F. Steenhuisen, and S. Wilson (2006), Global anthropogenic mercury emission inventory for 2000, *Atmos. Environ.*, *40*, 4048–4063, doi:10.1016/j.atmosenv.2006.03.041.

Pickard, G., and W. Emery (1990), *Descriptive Physical Oceanography*, 5th ed., 320 pp., Elsevier Sci., Woburn, Mass.

Redfield, A. C., B. H. Ketchum, and F. A. Richards (1963), The influence of organisms on the composition of sea-water, in *The Sea*, vol. 2, edited by M. N. Hill, pp. 26–77, Interscience, New York.

Sabine, C. L., R. A. Feely, F. J. Millero, A. G. Dickson, C. Langdon, S. Mecking, and D. Greely (2008), Decadal changes in Pacific carbon, *J. Geophys. Res.*, *113*, C07021, doi:10.1029/2007JC004577.

Schlitzer, R. (2004), Export production in the equatorial and North Pacific derived from dissolved oxygen, nutrient and carbon data, *J. Oceanogr.*, *60*, 53–62, doi:10.1023/B:JOCE.0000038318.38916.e6.

Selin, N. E., and D. J. Jacob (2008), Seasonal and spatial patterns of mercury wet deposition in the United States: Constraints on the contribution from North American anthropogenic sources, *Atmos. Environ.*, *42*, 5193–5204, doi:10.1016/j.atmosenv.2008.02.069.

Selin, N. E., D. J. Jacob, R. J. Park, R. M. Yantosca, S. Strode, L. Jaegle, and D. Jaffe (2007), Chemical cycling and deposition of atmospheric mercury: Global constraints from observations, *J. Geophys. Res.*, *112*, D02308, doi:10.1029/2006JD007450.

Selin, N. E., D. J. Jacob, R. M. Yantosca, S. Strode, L. Jaegle, and E. M. Sunderland (2008), Global 3-D land-ocean-atmosphere model for mercury: Present-day versus preindustrial cycles and anthropogenic enrichment factors for deposition, *Global Biogeochem. Cycles*, *22*, GB2011, doi:10.1029/2007GB003040.

St. Louis, V. L., H. Hintelmann, J. A. Graydon, J. L. Kirk, J. Barker, B. Dimock, M. J. Sharp, and I. Lehnherr (2007), Methylated mercury species in Canadian high Arctic marine surface waters and snowpacks, *Environ. Sci. Technol.*, *41*, 6433–6441, doi:10.1021/es070692s.

Strode, S., L. Jaegle, N. E. Selin, D. J. Jacob, R. J. Park, R. M. Yantosca, R. P. Mason, and F. Slemr (2007), Air-sea exchange in the global mercury cycle, *Global Biogeochem. Cycles*, *21*, GB1017, doi:10.1029/2006GB002766.

Strode, S., L. Jaegle, D. Jaffe, P. Swartzendruber, N. E. Selin, C. Holmes, and R. M. Yantosca (2008), Trans-Pacific transport of mercury, *J. Geophys. Res.*, *113*, D15305, doi:10.1029/2007JD009428.

Sunderland, E. M. (2007), Mercury exposure from domestic and imported estuarine and marine fish in the U.S. seafood market, *Environ. Health Perspect.*, *115*(2), 235–242.

Sunderland, E. M., and R. P. Mason (2007), Human impacts on open ocean mercury concentrations, *Global Biogeochem. Cycles*, *21*, GB4022, doi:10.1029/2006GB002876.

Sunderland, E. M., F. A. P. C. Gobas, A. Heyes, B. A. Branfireun, A. K. Bayer, R. E. Cranston, and M. B. Parsons (2004), Speciation and bioavailability of mercury in well-mixed estuarine sediments, *Mar. Chem.*, *90*, 91–105, doi:10.1016/j.marchem.2004.02.021.

Sunderland, E. M., F. A. P. C. Gobas, B. A. Branfireun, and A. Heyes (2006), Environmental controls on the speciation and distribution of mercury in coastal sediments, *Mar. Chem.*, *102*, 111–123, doi:10.1016/j.marchem.2005.09.019.

Takahashi, T., W. S. Broecker, and S. Langer (1985), Redfield ratio based on chemical data from isopycnal surfaces, *J. Geophys. Res.*, *90*, 6907–6924, doi:10.1029/JC090iC04p06907.

Talley, L. (1993), Distribution and formation of North Pacific Intermediate Water, *J. Phys. Oceanogr.*, *23*, 517–537, doi:10.1175/1520-0485(1993)023<0517:DAFONP>2.0.CO;2.

Ueno, H., and I. Yasuda (2003), Intermediate water circulation in the North Pacific subarctic and northern subtropical regions, *J. Geophys. Res.*, *108*(C11), 3348, doi:10.1029/2002JC001372.

Ueno, H., E. Oka, T. Suga, H. Onishi, and D. Roemmich (2007), Formation and variation of temperature inversions in the eastern subarctic North Pacific, *Geophys. Res. Lett.*, *34*, L05603, doi:10.1029/2006GL028715.

Warner, M., and R. Weiss (1985), Solubilities of chlorofluorocarbons 11 and 12 in water and seawater, *Deep Sea Res.*, *32*(12), 1485–1497, doi:10.1016/0198-0149(85)90099-8.

Watanabe, Y., A. Shimamoto, and T. Ono (2003), Comparison of time-dependent tracer ages in the western North Pacific: Oceanic background levels of SF6, CFC-11, CFC-12 and CFC-113, *J. Oceanogr.*, *59*, 719–729, doi:10.1023/B:JOCE.0000009600.12070.1a.

Weiss, R. (1970), The solubility of nitrogen, oxygen and argon in water and seawater, *Deep Sea Res.*, *17*, 347–359.

Whalin, L., E.-H. Kim, and R. P. Mason (2007), Factors influencing the oxidation, reduction, methylation and demethylation of mercury species in coastal waters, *Mar. Chem.*, *107*, 278–294, doi:10.1016/j.marchem.2007.04.002.

Wiener, J., D. P. Krabbenhoft, G. Heinz, and A. Sheuhammer (2003), Ecotoxicology of mercury, in *Handbook of Ecotoxicology*, 2nd ed., edited by D. J. Hoffman et al., pp. 407–461, CRC Press, Boca Raton, Fla.

Wilson, S., F. Steenhuisen, J. Pacyna, and E. Pacyna (2006), Mapping the spatial distribution of global anthropogenic mercury atmospheric emission inventories, *Atmos. Environ.*, *40*, 4621–4632, doi:10.1016/j.atmosenv.2006.03.042.

Wisegarver, D., and R. Gammon (1988), A new transient tracer: Measured vertical distribution of CCl2FCClF2 (F-113) in the North Pacific Subarctic Gyre, *Geophys. Res. Lett.*, *15*(2), 188–191, doi:10.1029/GL015i002p00188.

D. P. Krabbenhoft, U.S. Geological Survey, 8505 Research Way, Middleton, WI 53562, USA. (dpkrabbe@usgs.gov)

W. M. Landing, Department of Oceanography, Florida State University, 117 North Woodward Avenue, Tallahassee, FL 32306, USA. (wlanding@fsu.edu)

J. W. Moreau, School of Earth Sciences, University of Melbourne, Melbourne, AU VIC 3010, Australia. (jmoreau@unimelb.edu.au)

S. A. Strode, Department of Atmospheric Sciences, University of Washington, Seattle, Washington, WA 98195, USA. (sarahstrode@gmail.com)

E. M. Sunderland, School of Engineering and Applied Sciences, Harvard University, 29 Oxford Street, Cambridge, MA 02138, USA. (ems@seas.harvard.edu)